AoB PLANTS, 2024, **16**, plae009
https://doi.org/10.1093/aobpla/plae009
Advance access publication 28 February 2024
Tools

Tools

Development and application of an inexpensive open-source dendrometer for detecting xylem water potential and radial stem growth at high spatial and temporal resolution

Sean M. Gleason[*,1,2], Jared J. Stewart[1,3], Brendan Allen[1,2], Stephanie K. Polutchko[1,3], Jordan McMahon[1,4], Daniel Spitzer[2] and David M. Barnard[1]

[1]Water Management and Systems Research Unit, USDA-ARS, Fort Collins, CO 80526, USA
[2]Department of Forest and Rangeland Stewardship, Colorado State University, Fort Collins, CO 80523, USA
[3]Department of Ecology and Evolutionary Biology, University of Colorado, Boulder, CO 80309, USA
[4]College of Engineering, Science, Technology, and Agriculture, Central State University, Wilberforce, OH 45384, USA

[*]Corresponding author's e-mail address: sean.gleason55@gmail.com

Associate Editor: Kate McCulloh

Abstract. There is currently a need for inexpensive, continuous, non-destructive water potential measurements at high temporal resolution (<1 min). We describe here the development and testing of an entirely open-source dendrometer that, when combined with periodic Scholander pressure chamber measurements, provides sub-minute resolution estimates of water potential when placed on tissues exhibiting little or no secondary growth (petioles, monocotyledon stems). The dendrometer can also be used to measure radial growth of stems and branches when placed on dicotyledon and gymnosperm species. The dendrometer can be interfaced directly with a computer in real time in the lab or greenhouse, or connected to a datalogger for long periods of use in the field on batteries. We tested this device on a herbaceous dicotyledon (*Helianthus annuus*) (petioles and stems) and a monocotyledon (*Zea mays*) species (stems) for 1 week during dehydration and re-watering treatments under laboratory conditions. We also demonstrated the ability of the device to record branch and trunk diameter variation of a woody dicotyledon (*Rhus typhina*) in the field. Under laboratory conditions, we compared our device (hereafter 'contact' dendrometer) with modified versions of another open-source dendrometer (the 'optical' dendrometer). Overall, contact and optical dendrometers were well aligned with one another, with Pearson correlation coefficients ranging from 0.77 to 0.97. Both dendrometer devices were well aligned with direct measurements of xylem water potential, with calibration curves exhibiting significant non-linearity, especially at water potentials near the point of incipient plasmolysis, with pseudo R^2 values (Efron) ranging from 0.89 to 0.99. Overall, both dendrometers were comparable and provided sufficient resolution to detect subtle differences in stem water potential (ca. 50 kPa) resulting from light-induced changes in transpiration, vapour pressure deficit and drying/wetting soils. All hardware designs, alternative configurations, software and build instructions for the contact dendrometers are provided.

Keywords: Arduino; dendrometer; dicotyledon; micro-controller; monocotyledon; water potential.

Introduction

Many routine plant physiological methods depend on accurate and timely measurements of xylem water potential, that is, the potential energy of water within intact xylem tissue. Water potential measurements are critical for understanding and quantifying water movement, tissue desiccation and damage (i.e. 'stress'), as well as the physiological functioning of organelles, whole tissues and whole plants. Although plant physiologists have been measuring xylem water potential with thermocouple psychrometers since the late 1950s (Monteith and Owen 1958; Richards and Ogata 1958), these methods still require difficult installation and calibration procedures, are unsuitable for many species/organs (e.g. most grasses, leaves), and require relatively long equilibration times. Furthermore, thermocouple psychrometers are prohibitively expensive for many labs and researchers, with individual units costing in excess of 4000 US dollars. A trusted alternative to thermocouple psychrometry was offered in the form of the Scholander pressure chamber (Scholander *et al.* 1965), and although this method has become a mainstay in plant physiology labs worldwide, it is both relatively slow and destructive, and thus largely unsuitable for continuous/repeated measurements. Here, we describe an inexpensive electronic dendrometer (unit cost < 10 US dollars) that can provide non-destructive estimates of water potential at very high temporal and spatial resolution when combined with periodic direct measurements of xylem water potential (i.e. Scholander pressure chamber measurements).

Received: 28 September 2023; **Editorial decision:** 5 February 2024; **Accepted:** 26 February 2024

Hourly and daily variations in branch and stem diameter are often used to estimate plant water status for irrigation scheduling (Andales *et al.* 2006; Arbizu-Milagro *et al.* 2022) and plant growth/stress detection applications (Drew *et al.* 2011; Salomón *et al.* 2022). Underpinning their utility in these fields, fine temporal resolution dendrometer data reflect cambial activity, living cell turgor (e.g. cambium, phloem), xylem apoplast water potential and the thermal expansion of tissues (Daudet *et al.* 2004; Zweifel *et al.* 2005; Drew *et al.* 2011). Although this results in an 'integrated' biological and environmental measurement, the statistical or theoretical separation of these often confounded drivers is difficult or impossible, depending on the covariation among them, although there are procedures that can be applied, for example, separation of climate effects from growth (Rossi *et al.* 2003; Zweifel *et al.* 2005; Drew *et al.* 2022). A recent solution to this problem has been developed, where an 'optical' dendrometer (repeated imaging of a tissue with a fixed camera) is placed on leaf tips or leaf petioles, that is, tissues exhibiting no or limited secondary growth (Bourbia *et al.* 2021, 2022; Bourbia and Brodribb 2023). This method allows for continuous diameter (~water potential) measurements at sub-minute resolution and has been used to calculate transpiration and whole-root conductance (Bourbia *et al.* 2021, 2022) using the Whitehead–Jarvis proportionality (Whitehead *et al.* 1984) when combined with periodic Scholander pressure chamber measurements. The optical dendrometer has the added advantage of not being affected by thermal expansion of the device materials or electrical interference. A commercially available version of this optical dendrometer can also be purchased (https://cavicams.com/) at far less cost (~800 US dollars) than most thermocouple stem psychrometers, and modified/customized versions (see below) can be built for even less (raw materials per unit cost ~50 US dollars). Although do-it-yourself versions of the optical dendrometer, such as the types made for this study, will require focussing and image processing steps, which cannot be completely automated, and cannot be done at present using a micro-controller (computer and operating system are generally required), the commercially available version of the dendrometer has automated the focussing and image processing steps.

Here, we describe a dendrometer device consisting of a sliding variable resistor (i.e. potentiometer), similar to devices used in some commercial applications (Fig. 1). Under controlled conditions (e.g. growth chamber; Supporting Information—Fig. S1) our devices can achieve ca. 1 µm resolution and can be sampled at very short time steps (<1 s). Under less controlled conditions (e.g. field), the precision will depend on the potentiometer used (e.g. slide length, type), climate variation (temperature, wind, direct radiation), power source, components, etc. (details below).

Compared to similar, commercially available devices capable of the same level of spatial and temporal precision, the unique benefits of the device described here are:

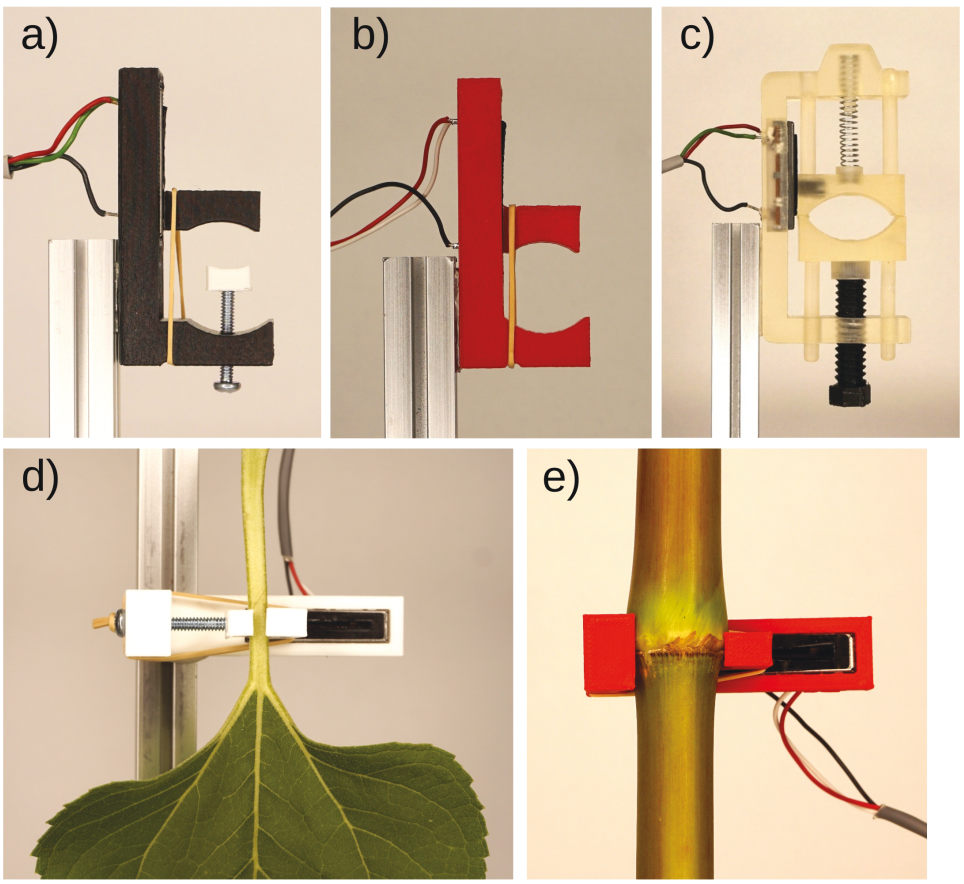

Figure 1. Contact dendrometer design and use. Adjustable PLA filament version of contact dendrometer requiring elastic bands (A), non-adjustable PLA filament version of contact dendrometer (B) and resin-printed compression spring design (C). Contact dendrometer placed on *Helianthus* petiole (D), and *Zea* stem (E).

(1) it can be built at very little cost (raw materials per unit cost < 10 US dollars) with open-source hardware and software, thus making them much more financially accessible to researchers and other users (e.g. irrigation managers)
(2) it can be operated using low power circuits and microcontrollers, allowing them to be run for long periods of time on small battery packs
(3) it requires no post-processing expertise or proprietary software to yield immediate diameter information
(4) it can be easily modified to suit just about any application because of its modular and versatile design
(5) the device is very quick and easy to install on plant petioles, twigs and stems

We note that the full realization of these benefits is dependent on some existing resources. For example, the manufacture of the device from its raw materials requires some tools (e.g. 3D printer, soldering iron). Likewise, building and programming the device requires some technical skill (e.g. general knowledge of C++, 3D printing, electronics), however, as these skills pertain to building and operating the device, they can typically be learned within a few weeks. Also, similar to all other dendrometer techniques, the device needs to be calibrated against periodic 'benchmark' water potential measurements using either a Scholander pressure chamber (preferred) or a thermocouple psychrometer.

Methods

Sensor and datalogger construction and operation

'Contact' sensor build. Contact dendrometers were made using non-brand 3-pin, 100 kΩ, sliding potentiometers purchased for ca. 0.50 US dollars per unit (Supporting Information—Table S1, Fig. 1). Although there are many different versions of potentiometers, we chose small 3-pin (35 × 5 mm) potentiometers for their light weight (5.0 g) and small size, as these would be suitable for attaching to both leaf petioles and plant stems. The 3-pin potentiometer used in our study (Fig. 1) functions as a voltage-dividing circuit. This is a simple circuit that converts a change in resistance, resulting from a change in the position of the lever (Fig. 1), to a change in voltage (change in electrical potential), which can then be measured by the datalogger (described below). Although the choice of sliding potentiometer is not important (maximal resistance, manufacturer), it is important to choose a size that is appropriate for the size of petiole/branch/stem that is measured. A sliding potentiometer that is too short will not fit on the organ, and one that is too long may not give the desired level of precision. Also, regardless of the maximum resistance of the potentiometer (e.g. 10 kΩ or 100 kΩ are most common), they should be fit with resistors on the + and – leads (pins 1 and 3) such that the minimal resistance is no less than ca. 10 kΩ. This will protect the analog-to-digital converter on the datalogger, protect against damage in the event the + and – leads are mislabelled or attached to the wrong screw terminals, reduce overall power consumption and allow for multiple potentiometers (sensors) to be wired to the same datalogger without interfering with one another. More information about potentiometers and voltage dividers can easily be found on several excellent online sources (e.g. Wikipedia, Instructables, ElectronicsHub).

Our dendrometer design requires petioles/stems to be lightly pinched, with tension being applied by either a small latex band or small compression spring (Fig. 1B and C) exerting ca. 1.0 N force. Given that the force applied by a spring/band is roughly proportional to the length it is extended/compressed (Hookes law), it is best to choose a dendrometer size and spring/band that allows significant expansion of the spring or band. For example, if the user expects ca. 2 mm change in diameter of a measured petiole, it is best to use a spring or band that can be extended at least 10 times this length (20 mm) to provide ca. 1 N of tension (or less) at the start of the experiment. Thus, if the stem were to increase or decrease by 2 mm, this would result in only a 10 % change in the force applied to the stem by the spring/band. Considering that it can be difficult to choose an elastic band for every situation (e.g. if different size stems need to be measured), the spring design is better because it allows for the adjustment of tension via a screw. Metal springs also do not deteriorate under ultraviolet light, unlike most elastic bands, which can result in small changes in applied force (see 'Results' section). Although the goals and conditions of the experiment will affect the choice of elastic band or spring used, it is best to apply the smallest force necessary to move the potentiometer lever and to spread this applied force over a large surface area, that is, the petiole/stem contact point.

Housings for the sensors were 3D printed using standard 1.5 mm polylactic acid (PLA) filament with a Lulzbot Taz 5 printer (Lulzbot, Fargo, ND, USA) (Fig. 1A and B), or else using transparent resin with a Creality Halot-Sky resin printer (Fig. 1C). 3D printer files are provided in the supplemental materials (SI materials). Dendrometers were interfaced with Arduino-based microprocessor dataloggers (described below) via 1.5 m of shielded, 3-strand, braided, 24 AWG cable (Alpha Wire Inc., Carmel, IN, USA) (Supporting Information—Table S1, Fig. 1). For this study, we built 12 dendrometers that interfaced with 3 dataloggers. Contact sensor data were interrogated and logged every 30 s.

Datalogger build. Various dataloggers can be fabricated to interface with the dendrometers. The version used in this study costs ca. 7 US dollars in parts and consists of (1) an Arduino Nano (brand name or 'clone'), (2) a 16-bit analog-to-digital (ADC) converter board, (3) 8 10 kΩ resistors, (4) 3 4-port, 2.54 mm screw terminals, (5) a PCB prototype board (ca. 30 × 70 mm), and (6) 22 AWG insulated solid-core copper wire (Supporting Information—Fig. S2A). This datalogger design allows data to be continuously streamed and plotted using a connected notebook or desktop computer running R software (R Core Team 2021). However, an SD card, LCD screen and digital clock can be added for little additional cost (ca. 5 US dollars) to allow for remote operation on batteries. Although this datalogger design can be built with many alternative components, we recommend using the same (or similar) I2C-compatible micro-controller (Arduino Nano) and ADC (ADS1115) to ensure the supplied controller sketch works without modification (Supporting Information—supplemental materials SI materials). Instructions for modifying our design, or building better designs, can be easily found on resources like Arduino Project Hub (https://www.arduino.cc/en/Tutorial/HomePage) and Instructables (https://www.instructables.com/Tools-and-Materials-for-Arduino/). Although we provide all our Arduino and R code for programming, communicating and collecting data for computers

running open-source LINUX-based operating systems (see Supporting Information), we note that this software can also be used on proprietary operating systems (e.g. MacOS, Windows) with slight modifications. We also note that our dendrometer devices can be easily interfaced with commercially available dataloggers (e.g. CR-1000X, Campbell Scientific Inc., Logan, UT, USA), or any device capable of measuring an analogue voltage signal (0–5 V) with at least 12-bit digital resolution.

Optical sensor build and modification. We compared the functioning of our 'contact' dendrometers against 'optical' dendrometers built after the recent design of Bourbia and Brodribb (2023) (https://cavicams.com/) (Supporting Information—Fig. S3A–H). Briefly, the optical dendrometer design measures changes in tissue size (e.g. petiole/stem diameter) by sequentially measuring the same organ repeatedly across a range of xylem water potentials. Similar to the contact dendrometer, the optical method requires either pressure chamber or thermocouple psychrometer benchmark measurements for calibration. Optical dendrometers were found to be strongly correlated with stem water potential under greenhouse (Bourbia *et al.* 2021, 2022) and field conditions (Bourbia and Brodribb 2023). Additionally, optical dendrometers do not require any physical contact with the petiole/stem being measured, although some physical contact is inevitable because the petioles/stems being measured need to be secured in a fixed position within the field of view. Optical dendrometers were built using 2MP OV2710 or Webcam Pro 9000 USB cameras (Arducam Technology Co., Kowloon, Hong Kong, PRC; Logitech Inc., Fremont, CA, USA) (Supporting Information—Fig. S3C), a PLA 3D printed housing and an LED MOSFET 'switchboard' (Supporting Information—Fig. S2B). Cameras and LEDs were controlled via OpenCV-Python (Bradski 2000). Optical dendrometer images were taken every 5 min on all instrumented plants.

Plant and climate measurements

We tested the efficacy of our dendrometer devices to estimate water potential (on *Helianthus annuus*, and *Zea mays*; hereafter '*Helianthus*' and '*Zea*') and record secondary stem growth (on *Helianthus*, and *Rhus typhina*; hereafter '*Rhus*') in both growth chamber (*Helianthus*, *Zea*) and under field conditions (*Rhus*). This allowed for a wide range of light, temperature and vapour pressure deficit (VPD) conditions, as well as testing across different plant functional types, that is, a herbaceous monocotyledon (*Zea*), a herbaceous dicotyledon (*Helianthus*) and a woody dicotyledon species (*Rhus*). To evaluate device sensitivity to fine-scale changes in light-induced transpiration, a growth chamber was specifically designed for this experiment to allow for the measurement of *Helianthus* and *Zea* plants, while also allowing for manipulation of light intensity under relatively constant temperature, soil moisture and humidity conditions (Supporting Information—Fig. S1). The growth chamber was equipped with three independently controlled LED light banks, each supplying ca. 200 µmol m^{-2} s^{-1} photosynthetic photon flux density (PPFD), measured every 10 min using a LI-190 quantum sensor and LI-6400XT gas exchange systems (LI-COR Biosciences, Lincoln, NE, USA). Relative humidity and air temperature were measured every 30 s using non-brand GY-SHT-31-D and AM2320 sensors, logged with an Arduino-based micro-controller board equipped with non-brand clock (DS3231) and SD card reader boards. Leaf temperature was measured every 30 s on the abaxial side of a single upper-story leaf on each plant (see below) with thermistors and logged using an Arduino-based micro-controller board interfaced with a notebook computer. Finally, whole-plant transpiration was measured by securing 25-µm thick polyethylene plastic over the soil surface of all pots and placing pots on continuously logging (30 s) scales (Adam CBK 70a, Adam Equipment Inc., Oxford, CT, USA).

Controlled conditions

Helianthus. *Helianthus annuus* cv. Mammoth plants were grown from seed (sown 24 February 2023) in a greenhouse (USDA Crops Research Laboratory, Fort Collins, CO, USA) with Philips GreenPower LED toplighting (Signify N.V.; Eindhoven, Netherlands) provided from 05:30 to 20:30. Thirteen plants were brought into the lab on 3 April 2023 when they were 38 days old (ca. 0.8 m height) and placed in a custom-built cage with the same lighting system (i.e. Philips GreenPower LED toplighting provided from 05:30 to 20:30; Supporting Information—Fig. S3). Our strategy for placing dendrometers on plants was firstly to ensure they were placed on the same/similar location on every plant. This was because we expected diameter variation to be strongly dependent on location along the stem/petiole, whereas we expected variation across the plants to be relatively small. Therefore, we tried to place every dendrometer on a different plant, rather than placing them on the same plant but at different locations, even if directly adjacent. However, given that we required several plants to sacrifice for water potential measurements, we were not able to do this in all cases (details below). Briefly, three contact dendrometers were placed on upper-canopy leaf petioles of three different plants. Four contact dendrometers were placed on the lower stems of four different plants ca. 15 cm from soil surface. Similarly, four optical dendrometers were placed on upper-canopy leaf petioles of four different plants, and four optical dendrometers were placed on the lower stems of four different plants. Although all petiole dendrometers were placed on independent plants, one contact and one optical dendrometer were placed on the same plant stem, with the contact dendrometer placed directly above and adjacent to the optical dendrometer (Supporting Information—Table S2). Additionally, three contact dendrometers were placed in the growth chamber to serve as controls, that is, they were not placed on plants but were allowed to vary over time. All contact dendrometers (including controls) were shielded from direct radiation by placing small aluminium foil disks directly above them. All pots were covered with polyethylene plastic as described above to prevent soil evaporation. To estimate whole-plant transpiration, two plants were placed on scales and logged every 30 s (1-g precision). From 3 April 2023 to 17 April 2023 plants were allowed to dry down to ca. −2.0 MPa stem water potential, re-watered (13 April 2023, at 19:30), and allowed to recover (video of dry down and recovery: https://www.youtube.com/watch?v=DdYC-3oFCO0).

Zea. *Zea mays* cv. B73 plants were grown from seed (sown 24 February 2023) in the greenhouse, and eight plants were brought into the lab on 17 April 2023 when they were 52 days old (ca. 1.3 m tall) and placed under lighting as described in the previous section. Four contact dendrometers were placed on the lower stems of four different plants, directly over the third node (from the base of the plant). Similarly, three of

the four plants instrumented with contact dendrometers were also instrumented with optical dendrometers, which were placed directly under the contact dendrometers. One optical dendrometer was placed on an independent plant at the same location as the other optical dendrometers. We also placed an additional contact dendrometer on the *upper* stem, directly over the fourth node (from the base of the plant), of an already instrumented plant ('lower' contact dendrometer). All pots were covered with polyethylene plastic as described above to prevent soil evaporation and all eight plants were placed on scales to measure whole-plant transpiration (30 s intervals, 1-g precision). From 28 April 2023 to 4 May 2023 plants were allowed to dry down to ca. –1.5 MPa water potential, re-watered (1 May 2023, at 21:30), and allowed to recover.

Rhus. Three contact sensors were placed on a single mature *R. typhina* tree growing in the field between 23 June 2023 and 8 July 2023, one sensor on the main stem (2.2 cm diameter), one on a secondary stem (1.7 cm diameter) and one on a terminal branch (1.0 cm diameter). Sensors were connected to an Arduino-based micro-controller datalogger equipped with a digital clock, LCD screen, and SD card and was powered by a deep-cycle 12 V marine battery. A fourth control sensor was also connected to the datalogger but was not affixed to the tree. All sensors were shielded from direct solar radiation using aluminium foil.

Sensor tests

Plant transpiration was modified by changing PPFD in the growth chamber in 200 µmol m^{-2} s^{-1} steps (i.e. 0, 200, 400 or 600 µmol m^{-2} s^{-1}) and maintaining each irradiance step for 2 h. This resulted in small differences in transpiration and proportional changes in water potential, which were then quantified using dendrometry (contact and optical) and benchmarked using a Scholander pressure chamber. Towards the end of each 2-h light treatment interval, pressure chamber measurements were taken on leaves that had been covered with custom-made polyethylene-aluminium foil bags for ca. 30 min to give an equilibrated stem water potential at each light step. Whole-plant transpiration and leaf-to-air VPD were measured simultaneously.

Data processing and analysis

Contact dendrometer data were corrected for control sensor noise (electromagnetic interference, thermal expansion of device materials), converted from mV to mm via a calibration curve (Supporting Information—Fig. S4), and plotted against time. Control sensor noise was accounted for by attaching a 'control' contact dendrometer to each datalogger. This control sensor was shaded from direct radiation using an aluminium foil disk, similar to the other sensors, but not installed on the plant. Variation in this sensor was removed from variation in the other non-control sensors at each time step, for example, at each time step variation in the control sensor was subtracted from variation in the other sensors. Calibration curves (mm ~ mV) were constructed using four different potentiometers (Supporting Information—Fig. S4). The potentiometers we purchased in bulk yielded a power function and were thus fit with a power model using the nlsLM function ($y \sim b \times x^c$), where y = change in diameter (mm) and x = change in mV (Efron r^2 = 0.994; relative standard error (RSE) = 0.354) (Supporting Information—Fig. S4). We note that although our potentiometers yielded a power function (with our resistor arrangement; Supporting Information—Fig. S5), most sliding resistors are likely to yield either linear or logarithmic (most common) output (distance ~ mV) and, thus, should be accounted for by fitting with an appropriate model.

Variation between dendrometers within groups (e.g. between contact dendrometers) and between groups (e.g. between contact and optical dendrometers) were evaluated using Pearson correlation coefficients. Two-parameter Weibull calibration models were fit for every dendrometer using Scholander pressure chamber measurements (MPa) taken on adjacent 'sacrifice' plants (dependent variable) and the fractional change (relative to full hydration) in petiole (*Helianthus*) or stem (*Zea* and *Helianthus*) diameter obtained for each dendrometer (independent variable). Pseudo R^2 statistics (Efron) were estimated as the sum of the squared model residuals, divided by the total variation in the dependent variable, to evaluate the overall goodness of fit. RSE was used to evaluate the relative fit within dendrometer group (contact, optical). We note that Efron pseudo R^2 values should be considered with some caution because R^2 values cannot be exactly calculated for non-linear models (e.g. sum of squares 'unity' problem) and are, therefore, not generally comparable to OLS models.

Images collected from the optical dendrometers were first thresholded to create binary black and white images, and then the mid-point diameter of each petiole/stem was measured in pixels using ImageJ software (Schneider *et al.* 2012). Changes in diameter (pixels) were then converted to mm using digital calliper measurements, and plotted against time. Reflections on stem and petiole surfaces and white-balance flickering required careful verification of the data after each image processing step to avoid large errors and to minimize noise. All data collection and analyses were performed on Debian-based (Linux) operating systems, running R (3.6.3) and RStudio (2023.06.1).

Results

Helianthus

There was good alignment among the contact dendrometers on petioles, with r values ranging from 0.957 to 0.972, as well as among the optical dendrometers, with r values ranging from 0.945 to 0.978 (Supporting Information—Table S2). Alignment between the contact and optical dendrometers that had been placed on petioles was slightly poorer, with r values ranging from 0.786 to 0.920 (Supporting Information—Table S2). Plotted against time, both contact and optical dendrometers captured the general diurnal trends in plant water status, with sharp declines in petiole diameter when overhead LED light banks were powered on, and either slightly increasing (optical) or no change (contact) in diameter when LED intensity was reduced (Fig. 2A). Optical dendrometers performed better in this respect, with small increases in night-time water potential being readily detected, whereas the contact dendrometers in most cases responded to increasing water potential only when it was sufficient to extend the latex band holding the sensor to the petiole, for example, the two dark periods following re-watering at the end of day 3 (Fig. 2A). Calibration models predicting water potential from the fractional change in petiole diameter (relative to full hydration) were markedly non-linear, especially

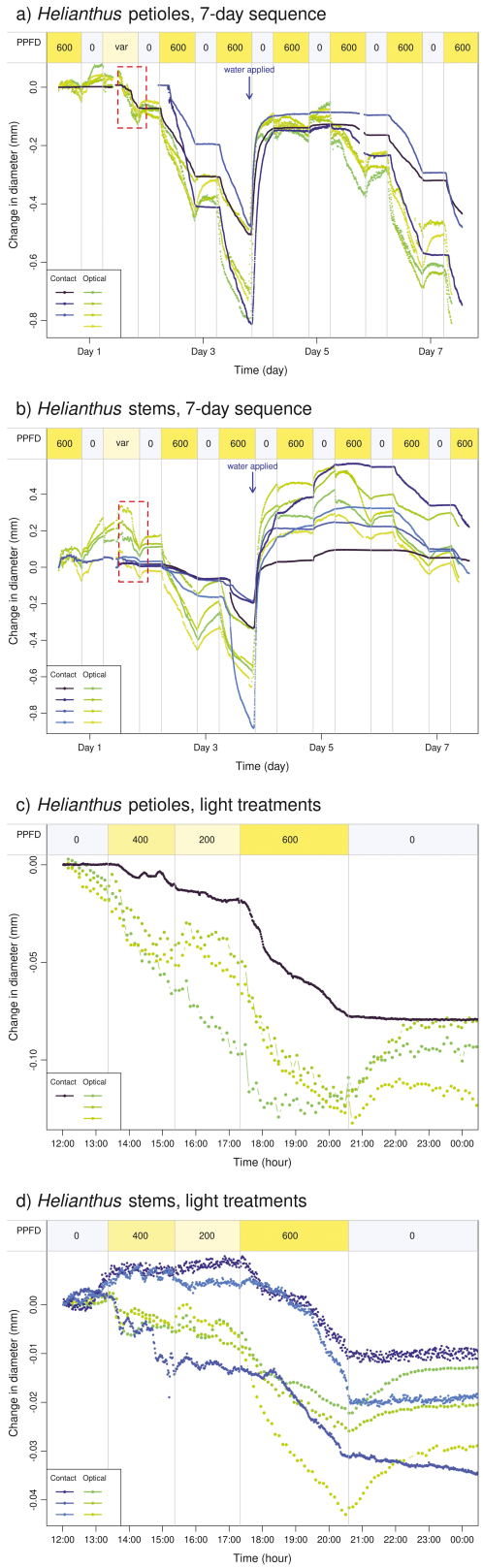

Figure 2. Time series plots of change in petiole (A and C) and stem (B and D) diameter of *Helianthus* plants over a 7-day experiment (A and B), and within two 12-h 'call-out' time periods (C and D). Call-out plot locations are represented by red boxes with broken borders (A and B). Plants were allowed to dry down during the experiment until they reached a xylem water potential of ca. −2.0 MPa when they were then re-watered (Day 4, 19:30 h) and allowed to recover until Day 7 without further watering. The light environment was manipulated during the call-out periods and is denoted at the top of each panel by colour (yellow, grey) and text indicating the PPFD. Change in diameter was started at zero for all dendrometers in all panels to maximize the visible detail for each trace. Thus the *y* axis scaling is not the same between dendrometer types (contact, optical) in all panels. Contact dendrometers are denoted with blue points and optical dendrometers are denoted with green points.

near the point of incipient plasmolysis (−0.7 to −1.0 MPa) (Jachetta *et al.* 1986; Cardoso *et al.* 2020) and exhibited little error and bias for both contact and optical methods (Fig. 3A and B). Stem diameter was consistent across all water potentials, whether water potential was increasing or decreasing, that is, little to no hysteresis (Fig. 3A and B).

Contact dendrometers placed on sunflower stems also exhibited a strong correlation, with *r* values ranging from 0.817 to 0.982, as did optical dendrometers, with *r* values ranging from 0.939 to 0.995 (Supporting Information—Table S2). Similar to dendrometers placed on petioles, alignment between contact and optical dendrometers placed on stems was slightly poorer, with *r* values ranging from 0.864 to 0.972 (Supporting Information—Table S2). Dendrometers placed on sunflower stems exhibited similar behaviour as dendrometers placed on petioles, with the most evident difference being the accumulation of radial growth, that is, wider stems at the end of the experiment than at the start (Fig. 2B). A subtle but interesting difference between the two dendrometer designs was the sharper decline (steeper slope and magnitude) during the day in the optical dendrometers versus the more gradual diameter decline of the contact dendrometers. Although this dynamic can be seen for both petiole and stem placements, it is most evident for devices placed on stems (Fig. 2B). Considering that much living tissue is present between the xylem cylinder and the cuticle (i.e. epidermal, cortical, phloem and cambial tissues), it is possible that these sharper declines in the optical sensor reflect not only water potential in xylem conduits and adjacent cells but also the loss of turgor pressure (~cell volume) in outer living cells.

Contact and optical dendrometers responded similarly to subtle differences in PPFD during the day, with declining stem diameter associated with increasing PPFD and increasing stem diameter associated with decreasing PPFD, for both petioles (Fig. 2C) and stems (Fig. 2D). Similar to the broader trends across days (Fig. 2A and B), optical dendrometers exhibited a sharper increase in diameter in response to lower PPFD, and especially when PPFD was reduced abruptly to zero (Fig. 2C and D).

Zea

Although contact and optical dendrometers exhibited fairly good alignment among and between dendrometer types (contact, optical), with *r* values ranging from (0.848 to 0.999) (Supporting Information—Table S2), *Zea* stems, in contrast to *Helianthus* stems, exhibited strong hysteresis, such that stems did not immediately return to their original diameter after experiencing water potentials below −2.0 MPa (Fig. 3C and D). Interestingly, when dendrometers were placed on nodes higher in the canopy (ca. above 'leaf' number 13), there was no hysteresis whatsoever, as we observed in a previously unpublished study, even when plants were dried well below their embolism points (Supporting Information—Fig. S6). Similar to *Helianthus*, optical dendrometers detected

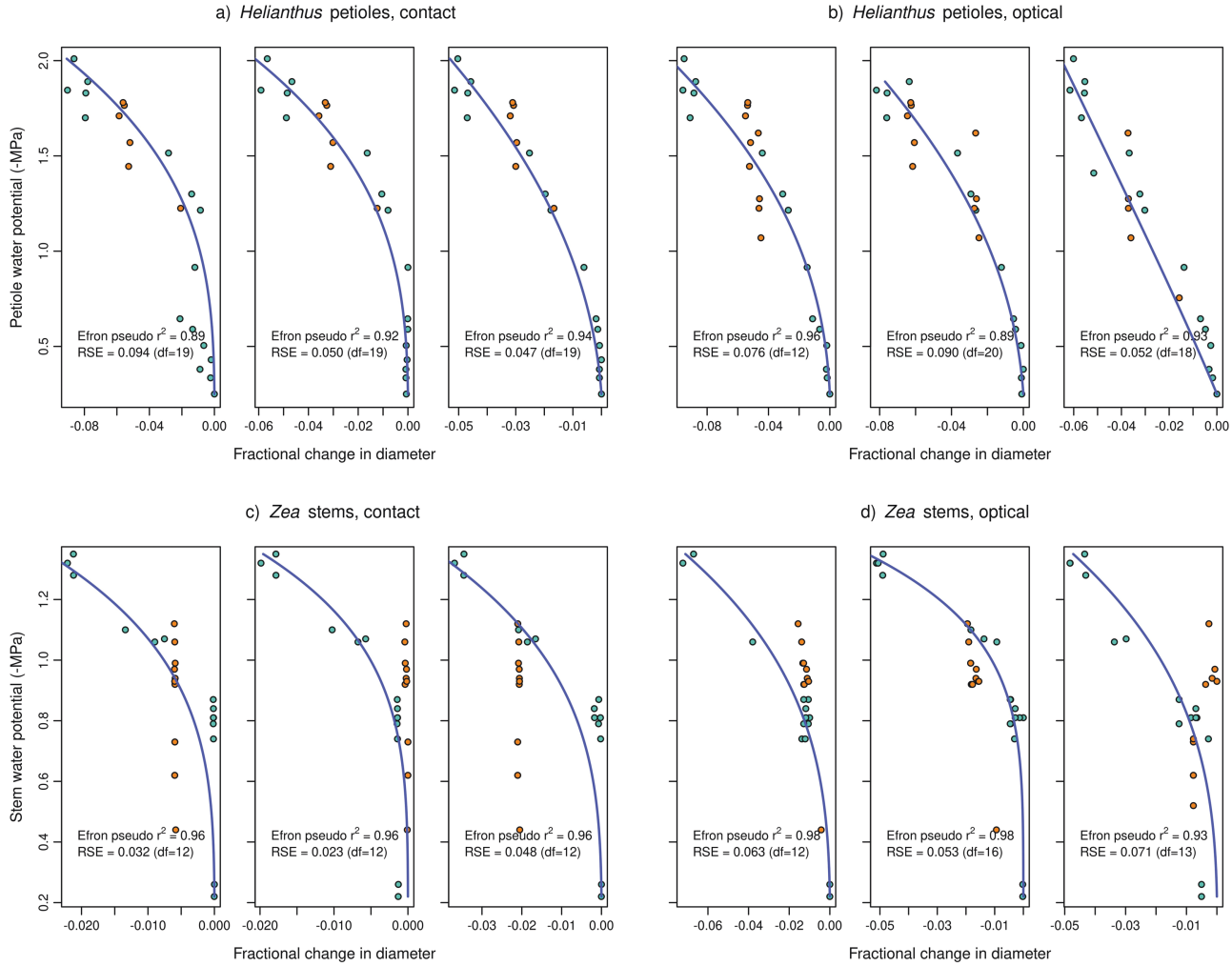

Figure 3. Water potential as a function of fractional change in diameter for *Helianthus* petioles (relative to full hydration) (A and B) and *Zea* stems (C and D). Contact (A) and optical (B) are denoted in the panel group subtitles, with each panel representing a different instrumented plant. Destructive water potential measurements were taken using a Scholander pressure chamber on adjacent 'sacrifice' plants of similar size to avoid sudden changes in water balance of plants instrumented with dendrometers. Thus, the same water potential measurements are plotted on the *y* axis for all panels of each species. Prior to measuring leaf water potential, leaves were allowed to equilibrate to stem water potential in shielded (aluminium foil) polyethylene bags for 30–60 min. Water potential measurements taken before and after re-watering are denoted with turquoise and orange symbols, respectively. *Helianthus* calibration models are fit to all data, whereas *Zea* calibration models are fit only to water potential measurements taken before re-watering (turquoise), owing to the marked hysteresis evident in this species after re-watering. Hysteresis in maize is evident in the near-vertical arrangements of points after watering. Although some maize stems eventually returned to their original size after re-watering, further water stress did not result in meaningful changes in diameter. In contrast, placing contract dendrometers higher on the stems, resulted in the absence of hysteresis, even when plants were dried down well below the embolism points (Supporting Information—Fig. S6).

slight increases in stem diameter occurring predominantly at night (Fig. 4A), but also in response to small (ca. 200 µmol m^{-2} s^{-1}) increases in PPFD (Fig. 4B and C). Night-time increases in stem diameter were observed with the optical dendrometers even at low stem water potentials (–1.4 MPa in *Zea* and –2.0 MPa in *Helianthus*). Qualitatively, contact dendrometers performed better at detecting small increases in stem diameter, in response to changing light conditions, later in the experiment (Fig. 4C) compared to earlier in the experiment (Fig. 4B). It is possible that this difference in contact dendrometer performance between the early and late stages of the experiment arose from the weakening of the elastic bands that were used to provide tension for the devices, that is, allowing for smaller increases in water potential (or turgor) to be detected. After omitting data following re-watering (Fig. 4A; after Day 4), models predicting water potential from the fractional change in stem diameter (relative to full hydration) were markedly non-linear, again near the point of incipient plasmolysis (–0.9 to –1.0 MPa) (Gleason *et al.* 2021) (Fig. 3C and D). Although Efron pseudo-R^2 values were quite high for all fitted calibration models (≥0.93), we note that much of the variation in water potential (*y* axis) can be attributed to the multiple plants that were pooled to obtain water potential estimates in both the sunflower and maize experiment, that is, multiple leaves could not be cut from plants instrumented with dendrometers without affecting their water balance, so adjacent plants of similar size were measured instead.

Rhus

The three contact dendrometers placed on *Rhus* stems in the field displayed predictable behaviour over the course of

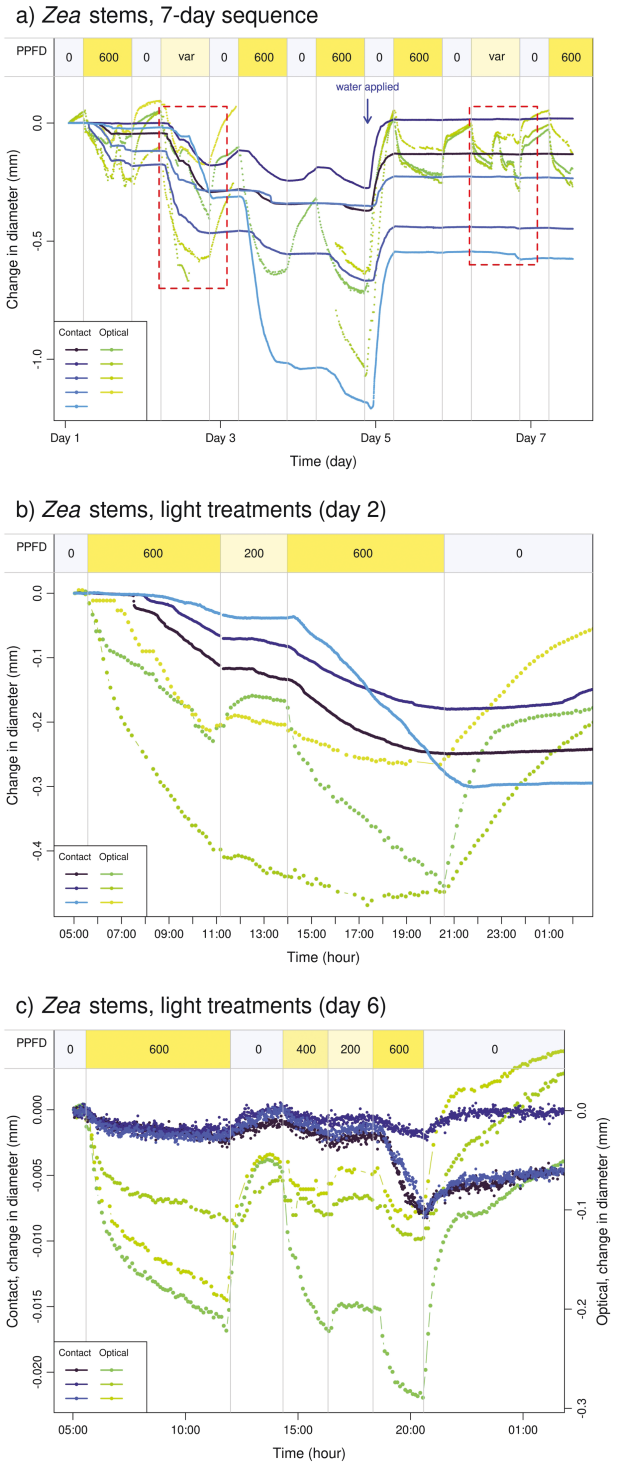

Figure 4. Time series plots of change in stem diameter of *Zea* plants over a 7-day experiment (A), and within two 12-h 'call-out' time periods (B and C). Call-out plot locations are represented by red boxes with broken borders (B and C). Plants were allowed to dry down during the experiment until they reached a xylem water potential of ca. −1.5 MPa when they were then re-watered (Day 4, 21:30 h) and allowed to recover until Day 7 without further watering. The light environment was manipulated during the call-out periods and is denoted at the top of each panel by colour (yellow, grey) and text indicating the PPFD. Change in diameter was started at zero for all dendrometers in all panels to maximize the visible detail for each trace. Thus the *y*-axis scaling is not the same between dendrometer types (contact, optical) in all panels. Contact dendrometers are denoted with blue points and optical dendrometers are denoted with green points.

14 days, with diurnal patterns of diameter following the expected variation in water potential, that is, low during the day and high during the night (Fig. 5). Additionally, all three dendrometers responded quickly to rainfall events occurring on June 30, July 4 and July 5 (Fig. 5). Although neither water potential nor optical measurements were taken during this time, this variation in stem diameter aligns with expected patterns of water use, water potential and radial stem growth, as reported previously (Sevanto *et al.* 2002; Daudet *et al.* 2004; De Swaef and Steppe 2010).

Discussion

Contact dendrometry for detecting stem water potential

Variation in leaf, petiole and stem size have been used previously as precise indicators of leaf and stem water potential (Huck and Klepper 1977; Sevanto *et al.* 2002; De Swaef and Steppe 2010; Vandegehuchte *et al.* 2014; De Swaef *et al.* 2015; Bourbia *et al.* 2021, 2022; Bourbia and Brodribb 2023). Therefore, our focus with this study was not to confirm the already reported relationship between diameter variation and water potential, but rather, to describe the development of an inexpensive sensor that would make high-resolution diameter measurement devices available to anyone with a need for diameter data, as well as traits that can be derived from these data. As such, the sensor, software and analysis tools required to collect and make sense of these measurements needed to be entirely open-source, free or inexpensive and straightforward to build, modify and share with others (e.g. code, files and design).

Within the context of our primary goals stated above, our sensors have several unique advantages and disadvantages that the builder/user should consider. Firstly, the diameter resolution obtained under both growth chamber and the field are similar to what is available from commercial sensors, but at a small fraction of the cost. The savings gained by building and using the sensors featured here, rather than commercially available sensors, can be invested back into the experiment, providing either a better spatial representation of plant function (e.g. more sensors on plants), or freeing resources for other measurements/analyses/expenses. It is also likely that the precision of the instrument could be improved by choosing higher quality components (e.g. potentiometers, resistors), 'cleaner' power sources or improving the circuit design (e.g. resistor, sensor, ADC arrangement). For example, experimenting with different potentiometers (brands, types, sizes, capacities), using temperature-stable resistors and other components (especially if used outdoors) and experimenting with different AC–DC transformers would likely improve on the described design. The second major advantage is the ease with which the hardware and software can be modified to whatever unique purpose is required. In contrast to this, sensor hardware purchased commercially cannot be easily modified (if at all), nor can the proprietary software required to interface, download and analyse data be accessed or altered (i.e. unfettered access to the uncompiled code) which, in our view, does not deliver the maximal utility of this technology to the end user.

The main disadvantage associated with the sensors described here, as well as commercially available contact sensors, is the contact force applied to the petiole/stem/trunk, which is

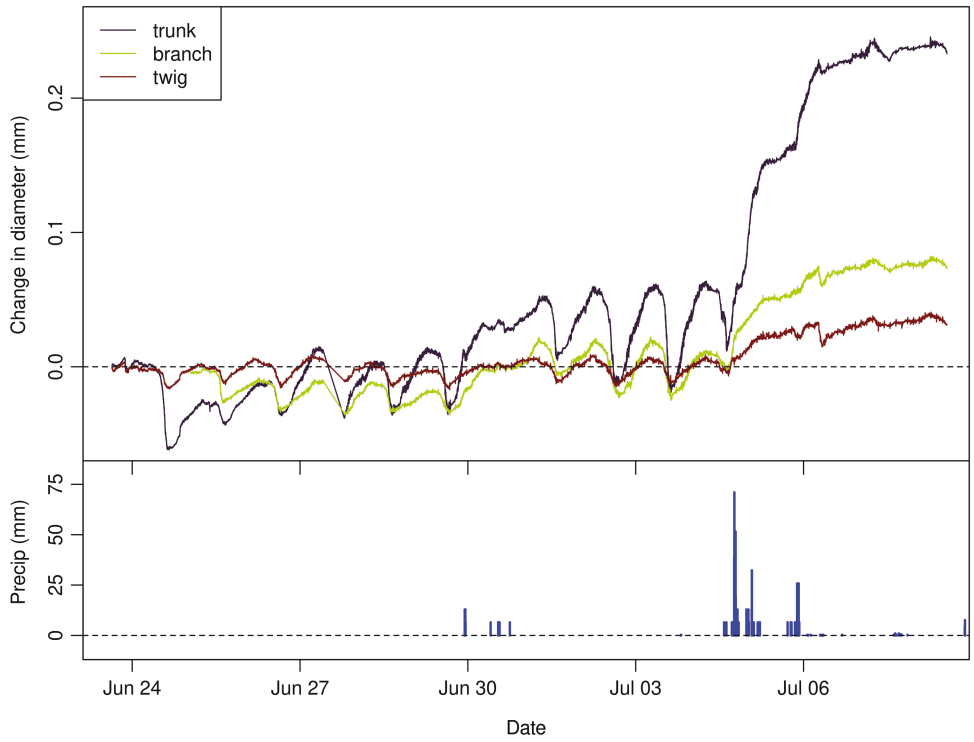

Figure 5. Time series plot of change in the trunk (2.2 cm; black), branch (1.7 cm; green) and twig (1.0 cm; red) diameter of a single *Rhus* plant during the course of a 14-day field experiment. Precipitation is plotted during this same period in the lower panel.

not an issue with either thermocouple psychrometers nor with the recently developed optical dendrometers (Bourbia *et al.* 2022). However, this may not be a disadvantage depending on the purpose of the device as well as the intended species, environment, and context to which it is applied. For example, the effects of small contact forces on plant tissues are likely to be negligible when small increases in water potential (ca. 0.1 MPa) are of no concern to the researcher, that is, most ecophysiological applications. Conversely, if small increases in water potential are important to the researcher (e.g. studies of osmotic adjustment or subtle changes to environmental conditions), then optical dendrometers would be a more appropriate choice. With respect to the optical dendrometer, it has a notable benefit over commercial thermocouple psychrometers of being entirely non-destructive and can be made via open-source hardware and software, or else can be purchased directly from the developers (https://cavicams.com/). The second important disadvantage of the contact sensors described here is that they do require some knowledge of micro-controller application, programming and 3D printing. However, considering that open-source micro-controller applications are becoming more important in ecophysiology and in the sciences more generally (Wenzel 2023), and that these skills can usually be learned in a few weeks, this 'disadvantage' may be an advantage to the researcher who obtains these skills while building their own sensors. A caveat to learning these skills too quickly is that mistakes and oversights will undoubtedly be made during the learning process, which could result in poorly functional devices. Also, unlike commercially available devices which have been made by professional engineers, our devices were made by biologists. As such, although our device and its performance from a biological stand point are sound, similar commercial devices are engineered to a higher standard.

Applications of dendrometry in the plant sciences

We see two key advantages to using dendrometers for quantifying water potential—high temporal sampling frequency (seconds) and sampling at multiple points across the same plant/organ. These advantages have already been leveraged to great effect for understanding wood synthesis (Drew *et al.* 2011), carbon and water budgets (Daudet *et al.* 2004; Chan *et al.* 2018), root and stem conductance (Bourbia *et al.* 2021), water use (Bourbia *et al.* 2022) and irrigation scheduling (Andales *et al.* 2006; Bourbia and Brodribb 2023). However, the application of dendrometry as a reliable proxy for xylem water potential is likely not as straightforward as we might wish. Firstly, there is little doubt that the direct contribution of xylem apoplastic pressure/volume on whole-petiole and whole-stem diameter is likely small relative to the contribution of water flux between the apoplast and living cells (Daudet *et al.* 2004). Given that passive and active (i.e. osmotic adjustment) water flux across plasma membranes is time-dependent, and likely occurs on time steps of minutes to hours (Matsuda and Riazi 1981; Morgan 1984; Steudle and Frensch 1996), very short measurement intervals of stem diameter (<1 min) may reflect rates of membrane conductance, rather than an equilibrated stem/petiole water potential. This time-dependent flux of 'capacitance' water into the transpiration stream is almost certainly what is responsible for long lags (>1 h) in stem diameter along the boles of large tree species (Offenthaler *et al.* 2001). However, this also highlights the potential usefulness of sub-minute and sub-second diameter measurements, especially considering that aquaporin-facilitated trans-membrane conductance in leaves can occur on these same short time intervals when leaves are sufficiently illuminated (Sack *et al.* 2002; Kim and Steudle 2009). As such, if apoplastic xylem water potential could be measured and compared with leaf

lamina, petiole and stem thickness at sub-second resolution, this would allow for the non-destructive separation of cell water volume flux from apoplastic pressure potentials. The efficacy of this method would also be dependent on the rate of cambial growth (dicotyledon/gymnosperm roots, stems) and organ expansion (e.g. leaves), which must be separated from water flux, or else determined to be negligible. Thus, the multiple confounded components of stem diameter variation warrant caution when interpreting dendrometer data, but also represent an opportunity to better understand plant diameter variation at different spatial and temporal scales.

Similarly, if combined with other emerging technologies (e.g. xylem μ-CT, nuclear magnetic resonance spectroscopy, genome-wide association studies), much could be learned about the role of water potential in the development of vascular and ground tissues, embolism and spread within and beyond the xylem apoplast, plant/tissue water balance and how genetic information and its transcription might be modified to improve food and wood production. It is our hope that the information provided here and in the supplemental materials will be used to improve the described sensors as well as the current applications for which they are currently being used.

Supporting Information

The following additional information is available in the online version of this article –

Table S1. Parts, equipment, and software list for constructing contact dendrometers.

Table S2. Pearson correlation coefficients among all contact dendrometers and optical dendrometers placed on *Helianthus* petioles/stems and *Zea* stems.

Figure S1. Growth cage setup during *Helianthus* controlled environment experiment.

Figure S2. Arduino Nano micro-controller board used to interface four contact dendrometers to a computer.

Figure S3. Optical dendrometer design and use.

Figure S4. Calibration model predicting the linear displacement of potentiometer as a function of voltage.

Figure S5. Circuit diagram for Arduino Nano microcontroller board.

Figure S6. Stem water potential vs. stem width calibration models for an unpublished maize study where contact dendrometers were placed higher on maize stems.

sup_data_all_dendro.csv: Raw data used in all figures and analyses.

Arduino (.ino) and R (.R) code files for interfacing four contact dendrometers and datalogger to a computer.

3D print files (.stl) and FreeCAD files (.FCStd) for printing and designing contact dendrometer parts.

Data Availability

All data used in this study are available for download from the supplemental information as a CSV file (sup_data_all_dendro.csv). All software needed for operating sensors, 3D prints, photos, and schematics have been included in the SI materials, and can also be freely accessed via github (https://github.com/sean-gl/dendrometer_water_potential_device).

Sources of Funding

J.J.S. was supported by an NSF Postdoctoral Research Fellowship in Biology, Grant No. IOS-1907338.

Acknowledgments

We would like to thank Amy Nielson for helping manage the greenhouse. We would also like to thank James Stewart and Carl Stewart for their help trouble shooting sensor and control board design, and Cameron Hunter for advice and assistance setting up the growth cage.

Contributions by the Authors

All authors contributed meaningfully to the manuscript. S.M.G., J.J.S., B.A., S.K.P. and J.M. designed the experiment and collected the data. S.M.G. wrote the first draft of the manuscript, and all other co-authors contributed to revisions and the final version.

Conflict of Interest Statement

None declared.

Literature Cited

Andales A, Wang J, Sammis TW, Mexal JG, Simmons LJ, Miller DR, Gutschick VP. 2006. A model of pecan tree growth for the management of pruning and irrigation. *Agricultural Water Management* 84:77–88.

Arbizu-Milagro J, Castillo-Ruiz FJ, Tascón A, Peña JM. 2022. How could precision irrigation based on daily trunk growth improve super high-density olive orchard irrigation efficiency? *Agronomy* 12:756.

Bourbia I, Brodribb TJ. 2023. A new technique for monitoring plant transpiration under field conditions using leaf optical dendrometry. *Agricultural and Forest Meteorology* 331:109328.

Bourbia I, Pritzkow C, Brodribb TJ. 2021. Herb and conifer roots show similar high sensitivity to water deficit. *Plant Physiology* 186:1908–1918.

Bourbia I, Lucani C, Brodribb TJ. 2022. Constant hydraulic supply enables optical monitoring of transpiration in a grass, a herb, and a conifer (J Zhang, Ed.). *Journal of Experimental Botany* 73:5625–5633.

Bradski G. 2000. The OpenCV library. *Dr. Dobb's Journal of Software Tools* 25:122–125.

Cardoso AA, Brodribb TJ, Kane CN, DaMatta FM, McAdam SAM. 2020. Osmotic adjustment and hormonal regulation of stomatal responses to vapour pressure deficit in sunflower (N Ruehr, Ed.). *AoB PLANTS* 12:plaa025.

Chan T, Berninger F, Kolari P, Nikinmaa E, Hölttä T. 2018. Linking stem growth respiration to the seasonal course of stem growth and GPP of Scots pine (M Ryan, Ed.). *Tree Physiology* 38:1356–1370.

Daudet F-A, Améglio T, Cochard H, Archilla O, Lacointe A. 2004. Experimental analysis of the role of water and carbon in tree stem diameter variations. *Journal of Experimental Botany* 56:135–144.

De Swaef T, Steppe K. 2010. Linking stem diameter variations to sap flow, turgor and water potential in tomato. *Functional Plant Biology* 37:429.

De Swaef T, De Schepper V, Vandegehuchte MW, Steppe K. 2015. Stem diameter variations as a versatile research tool in ecophysiology (D Way, Ed.). *Tree Physiology* 35:1047–1061.

Drew DM, Downes GM, Evans R. 2011. Short-term growth responses and associated wood density fluctuations in variously irrigated *Eucalyptus globulus*. *Trees* 25:153–161.

Drew DM, Allen K, Downes GM. 2022. Dynamics of seasonal growth in a long-lived southern hemisphere conifer are linked to early season temperature. *Dendrochronologia* 72:125933.

Gleason SM, Nalezny L, Hunter C, Bensen R, Chintamanani S, Comas LH. 2021. Growth and grain yield of eight maize hybrids are aligned with water transport, stomatal conductance, and photosynthesis in a semi-arid irrigated system. *Physiologia Plantarum* 172:1941–1949.

Huck MG, Klepper B. 1977. Water relations of cotton. II. Continuous estimates of plant water potential from stem diameter measurements[1]. *Agronomy Journal* 69:593–597.

Jachetta JJ, Appleby AP, Boersma L. 1986. Use of the pressure vessel to measure concentrations of solutes in Apoplastic and membrane-filtered Symplastic sap in sunflower leaves. *Plant Physiology* 82:995–999.

Kim YX, Steudle E. 2009. Gating of aqùaporins by light and reactive oxygen species in leaf parenchyma cells of the midrib of *Zea mays*. *Journal of Experimental Botany* 60:547–556.

Matsuda K, Riazi A. 1981. Stress-induced osmotic adjustment in growing regions of barley leaves. *Plant Physiology* 68:571–576.

Monteith JL, Owen PC. 1958. A thermocouple method for measuring relative humidity in the range 95-100%. *Journal of Scientific Instruments* 35:443–446.

Morgan JM. 1984. Osmoregulation and water stress in higher plants. *Annual Review of Plant Physiology* 35:299–319.

Offenthaler I, Hietz P, Richter H. 2001. Wood diameter indicates diurnal and long-term patterns of xylem water potential in Norway spruce. *Trees* 15:215–221.

R Core Team. 2021. *R: a language and environment for statistical computing*. https://www.r-project.org/ (3 March 2024).

Richards LA, Ogata G. 1958. Thermocouple for vapor pressure measurement in biological and soil systems at high humidity. *Science* 128:1089–1090.

Rossi S, Deslauriers A, Morin H. 2003. Application of the Gompertz equation for the study of xylem cell development. *Dendrochronologia* 21:33–39.

Sack L, Melcher PJ, Zwieniecki MA, Holbrook NM. 2002. The hydraulic conductance of the angiosperm leaf lamina: a comparison of three measurement methods. *Journal of Experimental Botany* 53:2177–2184.

Salomón RL, Peters RL, Zweifel R, Sass-Klaassen UGW, Stegehuis AI, Smiljanic M, Poyatos R, Babst F, Cienciala E, Fonti P, et al. 2022. The 2018 European heatwave led to stem dehydration but not to consistent growth reductions in forests. *Nature Communications* 13:28.

Schneider CA, Rasband WW, Eliceiri KW. 2012. NIH Image to ImageJ: 25 years of image analysis. *Nature Methods* 9:671–675.

Scholander PF, Bradstreet ED, Hemmingsen EA, Hammel HT. 1965. Sap pressure in vascular plants: negative hydrostatic pressure can be measured in plants. *Science* 148:339–346.

Sevanto S, Vesala T, Perämäki M, Nikinmaa E. 2002. Time lags for xylem and stem diameter variations in a Scots pine tree: time lags for xylem and stem diameter variations in Scots pine. *Plant, Cell & Environment* 25:1071–1077.

Steudle E, Frensch J. 1996. Water transport in plants: role of the apoplast. *Plant and Soil* 187:67–79.

Vandegehuchte MW, Guyot A, Hubeau M, De Swaef T, Lockington DA, Steppe K. 2014. Modelling reveals endogenous osmotic adaptation of storage tissue water potential as an important driver determining different stem diameter variation patterns in the mangrove species *Avicennia marina* and *Rhizophora stylosa*. *Annals of Botany* 114:667–676.

Wenzel T. 2023. Open hardware: from DIY trend to global transformation in access to laboratory equipment. *PLoS Biology* 21:e3001931.

Whitehead D, Edwards WRN, Jarvis PG. 1984. Conducting sapwood area, foliage area, and permeability in mature trees of *Picea sitchensis* and *Pinus contorta*. *Canadian Journal of Forest Research* 14:940–947.

Zweifel R, Zimmermann L, Newbery DM. 2005. Modeling tree water deficit from microclimate: an approach to quantifying drought stress. *Tree Physiology* 25:147–156.